

Document downloaded from:

<http://hdl.handle.net/10251/140840>

This paper must be cited as:

Tarrazó-Serrano, D.; Rubio Michavila, C.; Minin, OV.; Uris Martínez, A.; Minin, IV. (01-0).
Ultrasonic focusing with mesoscale polymer cuboid. *Ultrasonics*. 106:1-5.
<https://doi.org/10.1016/j.ultras.2020.106143>



The final publication is available at

<https://doi.org/10.1016/j.ultras.2020.106143>

Copyright Elsevier

Additional Information

ULTRASONIC FOCUSING WITH MESOSCALE POLYMER CUBOID

Daniel Tarrazó-Serrano⁽¹⁾, Constanza Rubio^{(1)*}, Oleg V. Minin^{(2), (3)}, Antonio Uris⁽¹⁾ and Igor V. Minin^{(2), (3)}

(1) Centro de Tecnologías Físicas: Acústica, Materiales y Astrofísica, Universitat Politècnica de València, Camino de Vera s/n, 46022 Valencia, Spain

(2) Tomsk Polytechnic University, 36 Lenin Avenue, Tomsk, 634050, Russia

(3) Tomsk State University, 30 Lenin Avenue, Tomsk, 634050, Russia

* Corresponding author: E-mail: crubiom@fis.upv.es

Abstract

In this paper, we demonstrate that, contrary to what the Geometrical Optics laws dictate, a flat polymer mesoscale cuboid immersed in water with no need of negative refraction can focus sound. Two main polymers were considered and lens parameters compared: PMMA and Rexolite®. It was concluded that Rexolite® is preferable for acoustic jet formation. The nature of the formation of the foci along the longitudinal axis, that is to say along the wave propagation axis, is numerically and experimentally demonstrated. In addition, the conditions under which a cubic particles lens of this type forms a single localized region with a sub-diffraction transverse size (approximately 0.44 wavelength) are determined. The comparisons of the acoustic wave pressures and the focal distance between the Finite Element Method based numerical results and the experimental results show fair agreement.

Keywords: acoustic beam, ultrasound, polymer mesoscale cuboid

1. Introduction

In the same way as a glass convex lens focuses light, an acoustic lens can focus sound waves. A key problem with this function is a factor known as acoustic impedance. Most of modern flat acoustic lenses are made from acoustic meta-surfaces. These are flat synthetic materials designed using building blocks smaller than the wavelength of the sound.

Yang et al [1] have demonstrated that a flat acoustic lens is possible by using a closed-packed face centered-cubic array of tungsten carbide beads embedded in water. Some [2, 3, 4] of the works referred to claimed that focusing by flat lens was due to the negative refraction property [5] of the corresponding phononic crystals. In the field of acoustic, sound focusing by non-conventional optical-type lenses were reported by Kock [6].

The design a flat sub-wavelength lens that can focus acoustic wave and made from an acoustic grating with curled slits was described in [7]. A new acoustic gradient-index metasurfaces engineered from soft graded-porous silicone rubber with a high acoustic index was offered by Y. Jin at al. [8] in applications to flat acoustic lens.

In the last years, the phenomenon of optical photonic jet [9-11] has attracted great attention not only because of the scientific interest of the phenomenon, but due to its potential applications in the design of optical sensors, tools for precision surgery, among other, in optics [9, 11-12], Terahertz imaging [10, 13-15], plasmonic [16, 17], etc. A photonic jet is a narrow beam with high intensity that emerges from the shadow surface of a dielectric particle, mainly cylinder or sphere, with diameters of several wavelengths, of the incident wave, and refractive index contrast, between the material and the surrounding medium, usually less than two [9,11]. It has been demonstrated that the waist of the photonic jets can be beyond the diffraction limit by varying the refractive index contrast and the size of a sphere [9, 11].

It is well known that both acoustic and electromagnetic waves share many phenomena. Therefore, studies developed for electromagnetic waves can be extended to acoustic waves, taking into account the intrinsic differences between them. One of the most significant examples are acoustic lenses, which are currently used in different areas ranging from engineering to medicine. Like optical lenses, acoustic lenses focus sound in the same way: using the phenomenon of diffraction or refraction. Thus, as in the optical case, in acoustics there are different types of acoustic lens designs: Fresnel lenses [18-20], lenses based on sonic crystals [21, 22] or on metamaterials [23-25].

Very recently, due to the analogy between electromagnetic and acoustic waves, the idea of a phononic jet, initially developed for electromagnetic waves, has been transferred to acoustic waves. O.V. Minin and I.V. Minin [26] demonstrated for the first time, through simulations, the existence of an acoustic analogy of the photonic jet phenomenon, which they called "acoustojet" (AJ). They observed the existence of an acoustic field localization in the shadow area of a penetrable sphere. The choice of material is a key problem due to the acoustic impedance and the existence of shear wave. In the case that there is not a significant difference between the material impedance and that of the surrounding medium, the intensity of the acoustic jet will be great. If materials with a big impedance difference with the surrounding medium are used, the intensity of AJ will be relatively low but, in this case reflection from the particle is large [27]. Taking these considerations into account, if the surrounding medium is water, there are polymer materials with a slight acoustic impedance difference with respect to water, such as cross-linking polystyrene with divinyl benzene (Rexolite®) [28].

It could be noted that Rexolite®, as an acoustic water immersed lens material, is usually used for high frequency, about 20-60 MHz, showing high phase velocity (almost constant=2315 m/s) and low attenuations (almost constant =2.2 dB/mm). But the application

of such polymer for low frequency acoustic lens operating at less than 10MHz has received little attention in the literature

The experimental demonstration of the acoustojet phenomenon [28] was performed in the ultrasonic range (1.01 MHz) using a Rexolite® sphere with diameter of 8 wavelength submerged in water. The observed transverse resolution of AJ was approximately 0.52 of wavelength in the surrounding medium, which is more than the diffraction limit. In the case of a cylindrical geometry, similar experimental results were also obtained [29].

From the geometric laws of Classical Physics it is well known, that for classical lens with refractive index more than 1 the curved surfaces are required to focus sound. In recent years, the appearance of acoustic metamaterials has made possible to obtain acoustic lenses with flat surfaces. However, the mechanization of metamaterials is sometimes difficult. Therefore, it would be interesting to obtain a flat acoustic lens attained from an easily machinable natural material.

This paper presents the experimental realization of an example of underwater solid polymer acoustical lenses obtained by acoustic jet principle. Here we demonstrate that sound focusing can be obtained by flat polymer mesoscale immersed in water with no need of negative refraction. We report on measurements of a subwavelength focusing of an ultrasound beam by a polymer cubic-shaped lens immersed in water at room temperature. Due to the low acoustic impedance contrast between water and Rexolite® and taking into account the results of [28], Rexolite® has been used. Rexolite® is a thermoset plastic produced by cross linking polystyrene with divinylbenzene. It has remarkable electrical properties and is frequently used in high-frequency circuit substrates, microwave components and in red-frequency and optical devices [30, 31]. It also can be easily machined. The results obtained with Rexolite® are compared with those obtained using polymethylmethacrylate (PMMA), that is a polymer that is commonly used in the manufacture of acoustic lenses [32].

There are two areas where the acoustic field is localized along longitudinal axis by cuboid particle-lens. The different nature of these two areas is discovered, discussed and experimentally verified. The focusing capacity of the cuboid is calculated by using the Finite Element Method (FEM). Furthermore, the influence of the size of the cuboid on the focalization is analyzed numerically as a function of the incident wavelength λ . Finally, it is shown for the first time that subwavelength single field localization less than diffraction limit is possible with flat surfaces. To validate the results of the FE simulations, experimental field plots of acoustic jets have been carried out for a range of lens configurations.

2. Numerical modelling and experimental set-up

The simulation results were obtained by using the commercial software COMSOL Multiphysics Modeling©. All the FEM models were solved with 3D modeling. **This first approximation model represents the ideal case of plane wave front propagation in water, normally incident on a cuboid of solid isotropic material.** The cuboid is located in a host medium. The contours of the host medium are defined as a radiation contour. This causes Sommerfeld's condition to be fulfilled, that is, no inward reflections occur. A plane-wave traverses this medium that contains the cube. Typical density rates and water propagation rates are considered. The host medium was water with typical sound speed (c) and density (ρ) values ($c_{\text{water}} = 1500 \text{ m s}^{-1}$ and $\rho_{\text{water}} = 1000 \text{ kg m}^{-3}$). In this case, host domain was solved with "Acoustic Module". The solid mechanics module is used to define the boundary and initial conditions of the cuboid. Rexolite® cuboid domain is defined as isotropic linear elastic material, determined by its longitudinal sound speed ($c_{\text{Rexolite}} = 2337 \text{ m s}^{-1}$), shear sound speed ($c_{\text{sRexolite}} = 1157 \text{ m s}^{-1}$), and density ($\rho_{\text{Rexolite}} = 1049 \text{ kg m}^{-3}$) [25-26]. The same type of cuboid has been selected in the case of PMMA material, but with changing its longitudinal sound speed ($c_{\text{PMMA}} = 2757 \text{ m s}^{-1}$), shear sound speed ($c_{\text{sPMMA}} = 1400 \text{ m s}^{-1}$), and density

($\rho_{\text{PMMA}} = 1200 \text{ kg m}^{-3}$) [32]. To obtain a consistent solution, the multiphysics module so called «Acoustic-Structure Boundary Conditions» that solves both modules with the perfect-coupling condition has been used. The working frequency defined for the simulation is 250 kHz. Due to it is a numerical model solved in FEM, the 3D model is discretized using by tetrahedral mesh type. To avoid numerical dispersion, the maximum element size was $\lambda/8$. To validate and verify the focusing properties of the cuboid, experimental measurements were made using the ultrasonic immersion transmission technique with a total precision automated measurement system. This system consisted of a fixed-piston ultrasonic transducer used as an emitter (Imasonic, Les Savourots, France) with a central frequency of 250 kHz and an active diameter of 0.032 m. As a receiver, a polyvinylidene fluoride needle hydrophone (PVDF) (model HPM1/1, precision acoustics Ltd., Dorchester, United Kingdom) with a diameter of 1.5 mm and a bandwidth of $\pm 4 \text{ dB}$ covering from 200 kHz to 15 MHz, was used. The piston transducer emitted pulses that were detected by the hydrophone. Afterwards, the signal was acquired, post-amplified and digitalized by digital oscilloscope for PC (model 3224 of Picoscope, Pico Technology, St. Neots, United Kingdom). The spatial resolution of the scanning system was $1 \times 1 \text{ mm}^2$. During the measurements, the water temperature was 18°C and the scanning was carried out with steps of 1 mm. The Rexolite® sample measured and the experimental set-up are shown in Figure 1. The cuboid was manufactured from a Rexolite® commercially available cylinder and it was machined using a numerical control milling machine.

3. Results and discussion

First, Figure 2 shows the simulated normalized sound pressure $\frac{|p|^2}{|p_i|^2}$ distributions (where p is the sound pressure and p_i is the incident sound pressure) for Rexolite® cuboids of five different sizes in XZ planes. As can be seen in Figure 2 (a), on the shadow surface of the

cuboid side 2λ appears the AJ, this is an acoustic field enhancement with a subwavelength focus. The Full Width at Half-Maximum (FWHM) in this case is 0.44λ (or 2.64 mm), where λ is the wavelength in water, $\lambda = 6$ mm. It is important to note that such a resolution of AJ is less than the diffraction limit ($\lambda/2n$) = 4.7 mm (where n is the refractive index contrast).

As the size of the cuboid edges increases (from 2λ to 4λ with steps of 0.5λ) the position of AJ varies, as shown in Figures 2 (b) - (e). Likewise, the FWHM of AJ also increases (see Table I). **For a mesoscale cubic particle, the mechanism of focus formation is due to two main effects. First, a wave inside a cubic particle near the edge propagates with a higher phase velocity than a wave in the center of the cube. Second, there is a curvature of the normally incident plane wavefront at the edge of the cuboid. Furthermore, this curvature is such that the wave is directed into the cuboid from the edges to the center. In this case, the two maxima of these waves converge at the center, forming a focus in the form of an acoustic jet.**

To explain this phenomenon, Figure 3 shows the simulated relative intensity ($\vec{I} = p \cdot \vec{v}$, where p is the sound pressure and \vec{v} is the particle velocity) flow diagrams in XZ planes for the different sizes of the cuboid considered. Figure 3 (a) shows that there are regions where the intensity lines produce vortices, in such a way the vortices (marked with circles) near the illuminated side of the cuboid redirect the intensity flow to different areas of the cuboid. As the size of the cuboid increases (see Figure 3 (b)) the distribution of these vortices varies, resulting in a redistribution of the energy inside the cuboid. It is observed that for the cuboid of size 3λ , the convergence of the intensity flow lines is maximum in certain areas of the interior near the shadow surface of the cuboid, giving rise to the formation of jets with lower pressure, greater FWHM and greater distance from the surface of the cuboid.

Another effect that can be observed is the formation of a secondary focus in the cuboid of size 3.5λ (see Figure 2 (d)), for distances around 4λ (3.89λ) and λ (0.74λ) from the shadow side of the cuboid. This secondary focus is formed due to the interference created by

the lateral lobes of the jet that become convergent for this size of the cuboid, the path difference for these distances is zero which satisfy the constructive interference condition. These interferences produce an enhancement of the normalized sound pressure $\frac{|P|^2}{|P_i|^2}$, being 4.02 and 2.73 at λ and 4λ distance, respectively. The values of FWHM and focus length of the secondary focus located at 4λ are 1.16λ and 6.06λ respectively. Finally, for a cuboid of size 4λ , focusing effect is observed at a distance of 8λ from the shadow side of the cuboid, and hence 12λ from the “illuminated” (front) side. This effect is created by the far-field obstacle diffraction due to the interference phenomenon of the secondary sources at the “illuminated” side according to the Huygens principle. To corroborate this fact, a simulation was carried out replacing the Rexolite® cube of size 4λ with a rigid solid cube of size 4λ . To ensure that there is no propagation of waves inside the cuboid, the rigid solid condition is used. As shown in Figure 4, it is clearly seen that the focusing effect at distance 8λ is due to diffraction.

Cuboid Side (λ)	2	2.5	3	3.5	4
FWHM (λ)	0.44	0.24	0.71	0.73	0.95
Acoustic Jet Length, L (λ)	1.12	0.32	1.28	0.96	1.88
$\frac{ P_{focus} ^2}{ P_{incident} ^2}$ (Pa²)	7.2	11.1	2.9	4.1	2.1

Table I. Full Width at Half-Maximum (FWHM), Acoustic Jet length (L) and $\frac{|P_{focus}|^2}{|P_{incident}|^2}$ as a function of cuboid size.

It is interesting to note that the effect of focusing with a wavelength-scaled particle in two foci is also valid for the optical band. Wu et al [33] propose a "superlong" photonic jet was where two maxima in the distribution of the field intensity along the jet are observed. However, the nature of this effect was not fully explored [33].

For comparison with Rexolite® cuboid, PMMA cuboids of edge size 2λ and 3λ are used. Figure 5 (a)-(b) show the simulated normalized sound pressure $\frac{|P|^2}{|P_i|^2}$ distributions in XZ planes for PMMA cuboids of 2λ and 3λ size respectively. As can be observed both in Figure 5(a) and Figure 5(b), on the shadow surface of the cuboids side appear the AJ at the same position. When comparing these results with those of the Rexolite® cuboids (see Figure 2) it is observed that in the case of the PMMA cuboid of size 3λ , the AJ is on the shadow surface of particle while in the case of Rexolite® cuboid, the AJ is out of shadow surface. Moreover, in the case of 3λ edge size PMMA cuboid, the second focus (due to scattering) is more visible but for Rexolite® cuboid it is not visible. It is important if we plan to apply this particle for single-focus device. To explain this different behavior, in Figure 5 (c) - (d) it is shown, the simulated relative intensity ($\vec{I} = p \cdot \vec{v}$) flow diagrams in XZ planes for cuboids of 2λ and 3λ size respectively. As can be seen, in the case of PMMA cuboids, the vortices are not found near the cuboid, unlike the Rexolite® cuboids, resulting in a different redistribution of the energy inside the cuboid. This fact is due to the different sound speed of the materials and more lower ratio of c_l / c_s for PMMA. So by selecting to materials properties, control of maximum pressure area position (jet) along z-axis is possible. In this case, unlike the PMMA cuboids, Rexolite® ones allow to vary the position of the maximum pressure area by varying the size of the cuboid.

To demonstrate and experimentally verify the acoustic focusing along the direction of acoustic wave propagation, we select a Rexolite® cuboid with an edge size of 3.5λ . From Figure 6 it can be seen that the simulated and experimental results agree well, which allows to validate the results of the simulations presented in this paper.

The possible discrepancies between the simulated and experimental results are due to the fact that the incident wave can not be guaranteed to be completely plane since, although

the cuboid was at a relatively long distance from the transducer, its emission is not really plane waves.

4. Conclusions

In this paper, the ultrasonic field localization produced by polymer cuboids lens immersed in water for low frequency has been investigated for the first time. As a polymer, Rexolite® has been used since it is a material with a low acoustic impedance difference with respect to water. By changing the edge size of the cuboid, it has been shown that the position of the acoustic jet varies, as does the FWHM. It has been observed and experimentally verified the appearance of effect of 2 foci farther from the cuboid and of a different nature. Such two-focusing acoustic particle-lens will greatly facilitate potential applications of far-field acoustic optics. It was also shown for the first time that it is possible to form subwavelength field localization near the shadow surface of 2λ metamaterial free cuboid lens with FWHM less than diffraction limit. The results have been compared with PMMA cuboids and it has been observed that the AJ appears at the same position on the shadow surface of the cuboids when the cuboid size varies. This effect is due to the different sound speed of the materials. So, control of maximum pressure area position along z-axis is possible by selecting to materials properties. Rexolite® is preferable polymer than PMMA in application to acoustic jet. The use of cuboids from a material such as Rexolite® is an inexpensive and easy way to obtain flat ultrasonic wavelength-scaled flat lenses. The potential applications of this type of particle-lens are varied and range from medical ultrasound to engineering applications and will be useful in the development of new ultrasonic devices, for example as a double co-propagating acoustical traps.

Acknowledgements

This work has been supported by Spanish Ministry of Science, Innovation and Universities (grant No. RTI2018-100792-B-I00). The research was partially supported by Tomsk Polytechnic University Competitiveness Enhancement Program.

References

- [1] S. Yang, J. H. Page, Z. Liu, M. L. Cowan, C. T. Chan, P. Cheng, Focusing of Sound in a 3D Phononic Crystal, *Phys. Rev. Lett.* 93 (2004), 024301.
- [2] X. Zhang, Z. Liu, Negative refraction of acoustic waves in two-dimensional phononic crystals, *Appl. Phys. Lett.* 85 (2004), 341.
- [3] L.-S. Chen, C.-H. Kuo, Z. Ye, Acoustic imaging and collimating by slabs of sonic crystals made from arrays of rigid cylinders in air, *Appl. Phys. Lett.* 85 (2004), 1072.
- [4] X. Hu, Y. Shen, X. Liu, R. Fu, J. Zi, Superlensing effect in liquid surface waves, *Phys. Rev. E* 69 (2004), 030201.
- [5] V. G. Veselago, The electrodynamics of substances with simultaneously negative values of ϵ and μ , *Sov. Phys. Usp.* 10 (1968), 509-513.
- [6] W. E. Kock, F. K. Harvey, Refracting Sound Waves, *J. Acoust. Soc. Am.* 21 (1949), 471.
- [7] P. Peng, B. Xiao, Y. Wu. Flat acoustic lens by acoustic grating with curled slits, *Phys. Lett. A*, 378(45) (2014), 3389-3392.
- [8] Y. Jin, R. Kumar, O. Poncelet, O. Mondain-Monval, T. Brunet, Flat acoustics with soft gradient-index metasurfaces, *Nat Commun.* 10 (2019), 143.
- [9] Heifetz A, Kong SC, Sahakian AV, Taflove A, Backman V, Photonic Nanojets. *J. Comput. Theor. Nanosci.* 6(9) (2009), 1979–1992.
- [10] L. Zhao, C. K. Onga, Direct observation of photonic jets and corresponding backscattering enhancement at microwave frequencies. *J. Appl. Phys.* 105 (2009), 123512.

- [11] B. S. Luk'yanchuk, R. Paniagua-Domínguez, I. V. Minin, O. V. Minin, Z. Wang, Refractive index less than two: photonic nanojets yesterday, today and tomorrow. *Opt. Mater. Express* 7 (2017), 1820-1847.
- [12] Z. Wang, W. Guo, L. Li, B. Lukyanchuk, A. Khan, Z. Liu, Z. Chen, M. Hong, Optical virtual imaging at 50 nm lateral resolution with a white-light nanoscope. *Nat. Commun.* 2 (2011), 218.
- [13] O.V. Minin, I.V. Minin, Terahertz artificial dielectric cuboid lens on substrate for super-resolution images. *Opt. Quant. Electron.* 49 (2017), 326-329.
- [14] H. H. Nguyen Pham, S. Hisatake, I.V. Minin, O.V. Minin, T. Nagatsuma, Three-dimensional direct observation of Gouy phase shift in a terajet produced by a dielectric cuboid. *Appl. Phys. Lett.* 108 (2016),191102.
- [15] H.-H. Nguyen Pham, S. Hisatake, Oleg V. Minin, T. Nagatsuma, I. V. Minin, Enhancement of Spatial Resolution of Terahertz Imaging Systems Based on Terajet Generation by Dielectric Cube. *APL Photonics* 2 (2017), 056106.
- [16] V. Pacheco-Peña, I. V. Minin, O. V. Minin, M. Beruete, Doubling the propagation distance of surface plasmon polaritons. *SPIE Newsroom* 102 (2016), 171109.
- [17] V. Pacheco-Peña, I. V. Minin, O. V. Minin, M. Beruete, Comprehensive analysis of photonic nanojets in 3D dielectric cuboids excited by surface plasmons. *Ann. Phys.* 528 (2016), 684-692.
- [18] D. C. Calvo, A. L. Thangawng, M. Nicholas, C. N. Layman, Thin Fresnel zone plate lenses for focusing underwater sound. *Appl. Phys. Lett.* 107 (2015), 114109.
- [19] X. Xia, F. Cai, F. Li, L. Meng, T. Ma, H. Zhou, M. Ke, C. Qiu, Z. Liu, H. Zheng, Planar Ultrasonic Lenses Formed by Concentric Circular Sandwiched-Ring Arrays. *Adv. Mater. Technol.* 4 (2019), 1800542.
- [20] M. Moleron, M. Serra-García, C. Daraio, Acoustic Fresnel Lenses with extraordinary transmission. *Appl. Phys. Lett.* 105 (2014), 114109.

- [21] F. Cervera, J.V. Sánchez-Pérez, R. Martínez-Sala, C. Rubio, F. Meseguer, C. Lopez, D. Caballero, J. Sánchez-Dehesa, Refractive acoustic device for airborne sound. *Phys. Rev. Lett.* 88 (2001) 023902.
- [22] A. Sukhovich, B. Merheb, K. Muralidharan, J.O.Vasseur, Y. Pennec, P.A. Deymier, J.H. Page, Experimental and Theoretical Evidence for Subwavelength Imaging in Phononic Crystals. *Phys. Rev. Lett.* 102 (2009), 154301.
- [23] Ma C, Aguinaldo, R, Liu Z, Advances in the hyperlens, *Chin. Sci. Bull.* 55 (2010), 2618.
- [24] X. Yang, J. Yin, G. Yu, L. Peng, and N. Wang, Acoustic superlens using Helmholtz-resonator-based metamaterials. *Appl. Phys. Lett.* 107 (2015),193505.
- [25] G. Y. Song, B. Huang, H. Y. Dong, Q. Cheng, T. J. Cui, Broadband Focusing Acoustic Lens Based on Fractal Metamaterials. *Sci. Rep.* 6 (2016), 35929.
- [26] O.V. Minin, I.V. Minin, Acoustic analogue of photonic jet phenomenon based on penetrable 3D particle. *Opt. Quant. Electron.* 49 (2017), 54.
- [27] J. H. Lopes, J. P. Leão-Neto, I. V. Minin, O. V. Minin, G. T. Silva, A theoretical analysis of jets. 22nd Int. Cong. Ac. (ICA 2016), Buenos Aires, 2016.
- [28] .H. Lopes, M.A.B. Andrade, J.P. Leao-Neto, J.C. Adamowski, I.V. Minin, G.T. Silva, Focusing Acoustic Beams with a Ball-Shaped Lens beyond the Diffraction Limit. *Phys. Rev. Appl.* 8 (2017), 024013.
- [29] I.V. Minin, O.V. Minin. Mesoscale acoustical cylindrical superlenses, MATEC Web of Conferences. EDP Sciences 155 (2018), 01029
- [30] C. Cadot, J.F. Saillant, B. Dulmet, Method for Acoustic Characterization of Materials in Temperature. *Proceed. 19th World Conf. on Non-Destruc. Tes. (WCNDT)*, Munich, 2016.
- [31] Lec Plastics Inc, <http://www.rexolite.com/general-qualities/>, accessed: March, 2019.

[32] W. Xia, D. Piras, J. C. G. van Hespén, W. Steenbergen, S. Manohar, A new acoustic lens material for large area detectors in photoacoustic breast tomography. *Photoacoustics* 1 (2013), 9-18.

[33] P. Wu, J. Li, K. Wei, W. Yue, Tunable and ultra-elongated photonic nanojet generated by a liquid-immersed core-shell dielectric microsphere. *Appl. Phys Express* 8 (2015), 112001.

FIGURE CAPTIONS

Figure 1. Detail of (a) Rexolite® sample measured and (b) experimental set-up.

Figure 2. Normalized sound pressure $\frac{|p|^2}{|p_i|^2}$ distributions in XZ planes for Rexolite® cuboids different sizes: (a) 2λ , (b) 2.5λ , (c) 3λ , (d) 3.5λ and (e) 4λ

Figure 3. Normalized relative intensity flow in XZ planes for Rexolite® cuboids different sizes: (a) 2λ (the inset corresponds to an enlargement of the illuminated face of the cuboid. Vortices are indicated in the circles), and (b) 3λ

Figure 4. Normalized sound pressure $\frac{|p|^2}{|p_i|^2}$ distribution in XZ planes for a solid rigid cuboid of edge size 4λ

Figure 5. Normalized sound pressure $\frac{|p|^2}{|p_i|^2}$ distributions in XZ planes for PMMA cuboids of edge size: (a) 2λ , (b) 3λ . Normalized relative intensity flow in XZ planes for PMMA cuboids of edge size: (c) 2λ and (d) 3λ .

Figure 6. Comparison of (a) simulated and (b) measured normalized sound pressure distribution in XZ planes for Rexolite® cuboid of 3.5λ size.

TABLE

Cuboid Side (λ)	2	2.5	3	3.5	4
FWHM (λ)	0.44	0.24	0.71	0.73	0.95
Acoustic Jet Length, L (λ)	1.12	0.32	1.28	0.96	1.88
$\frac{ P_{focus} ^2}{ P_{incident} ^2}$ (Pa²)	7.2	11.1	2.9	4.1	2.1

Table I. Full Width at Half-Maximum (FWHM), acoustic jet length (L) and $\frac{|P_{focus}|^2}{|P_{incident}|^2}$.

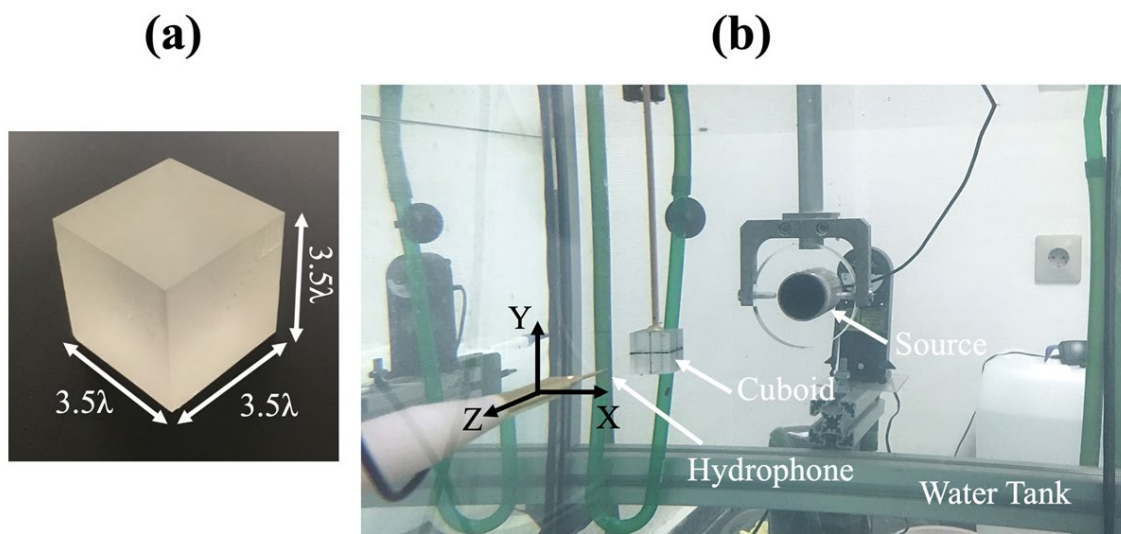


FIGURE 1

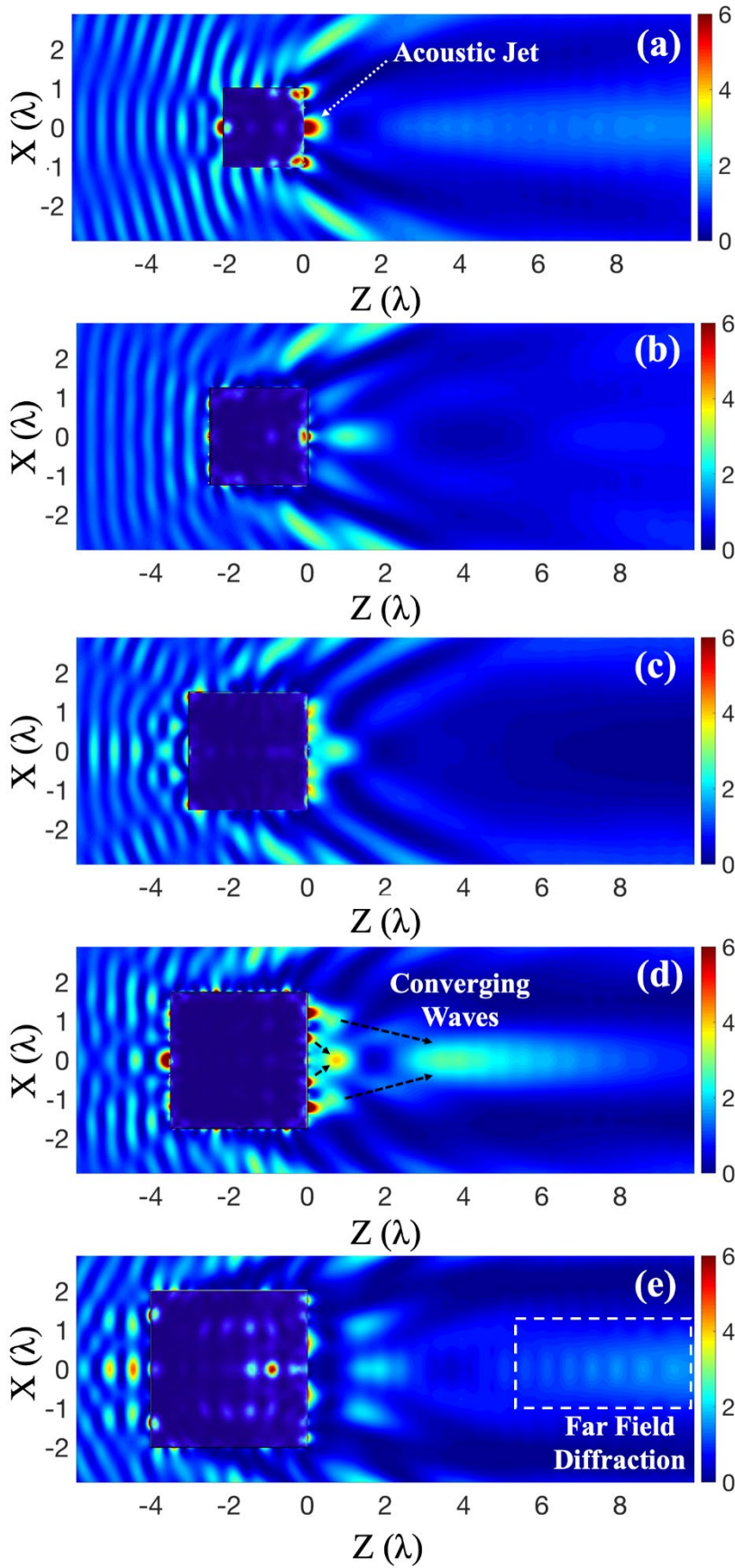


FIGURE 2

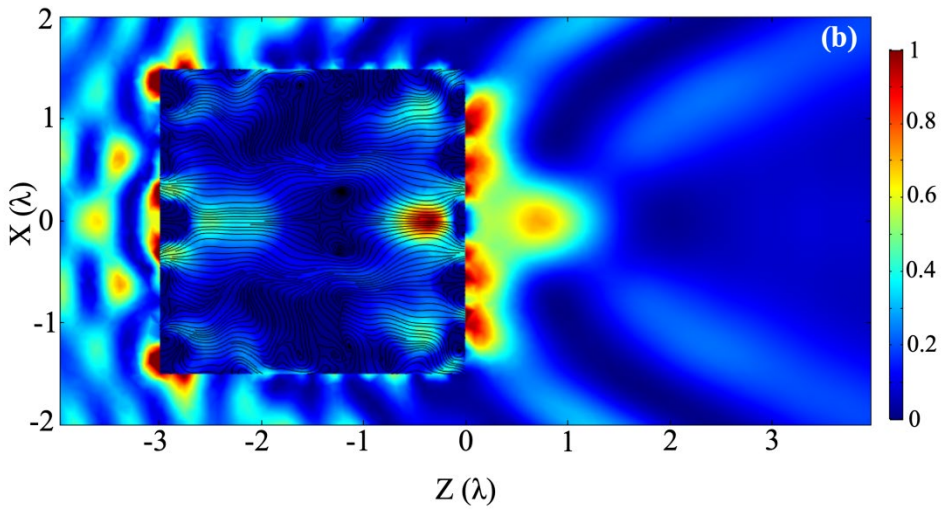
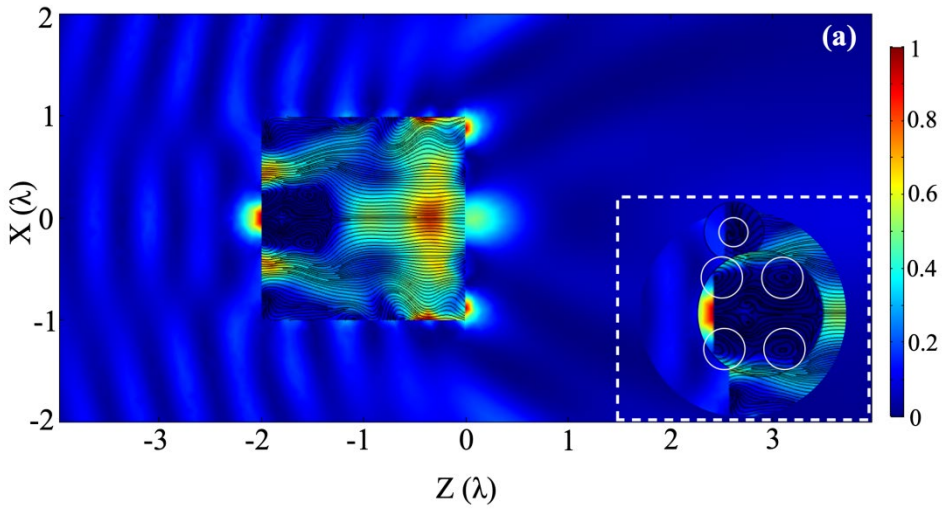


FIGURE 3

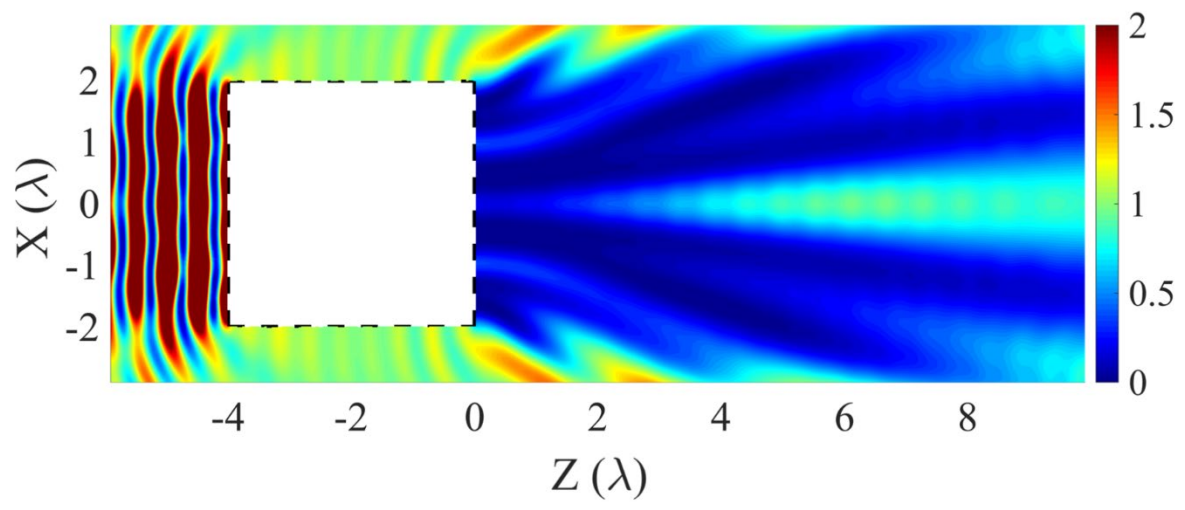


FIGURE 4

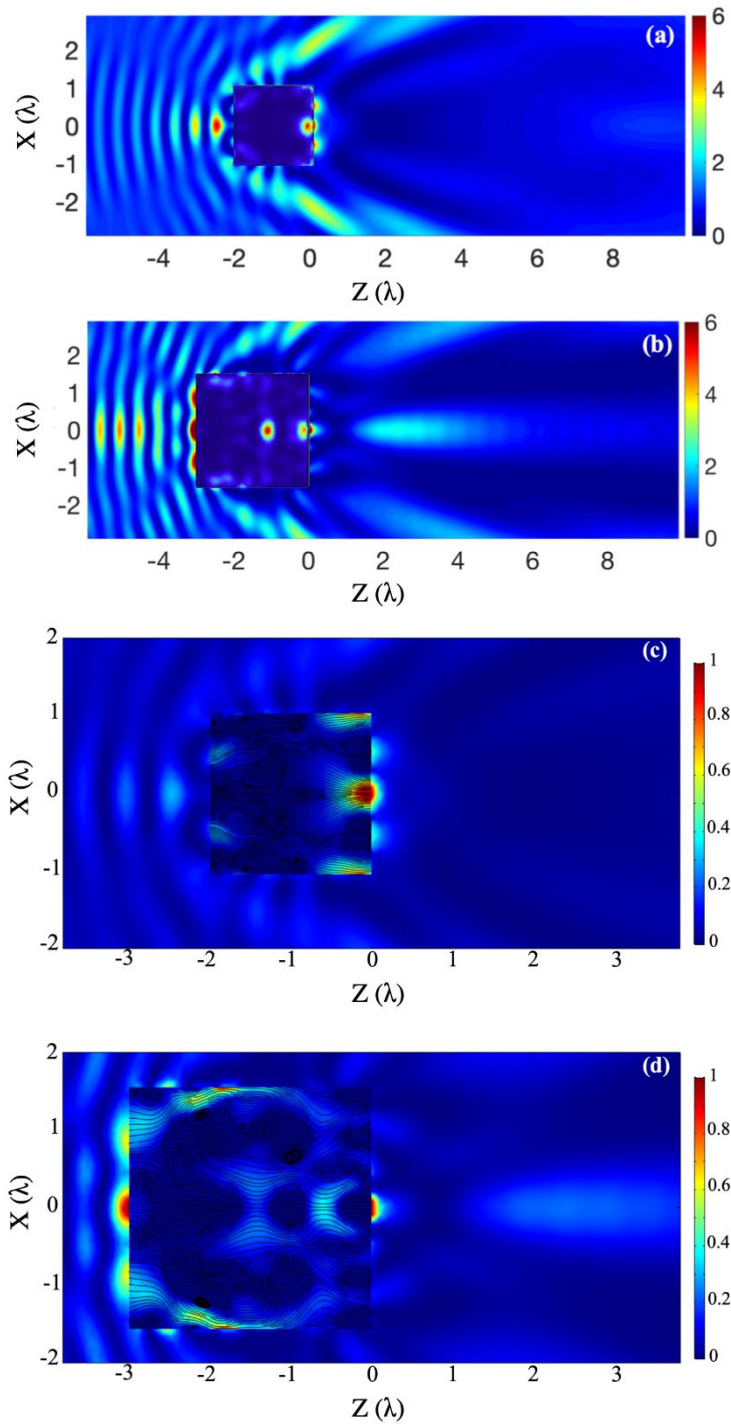


FIGURE 5

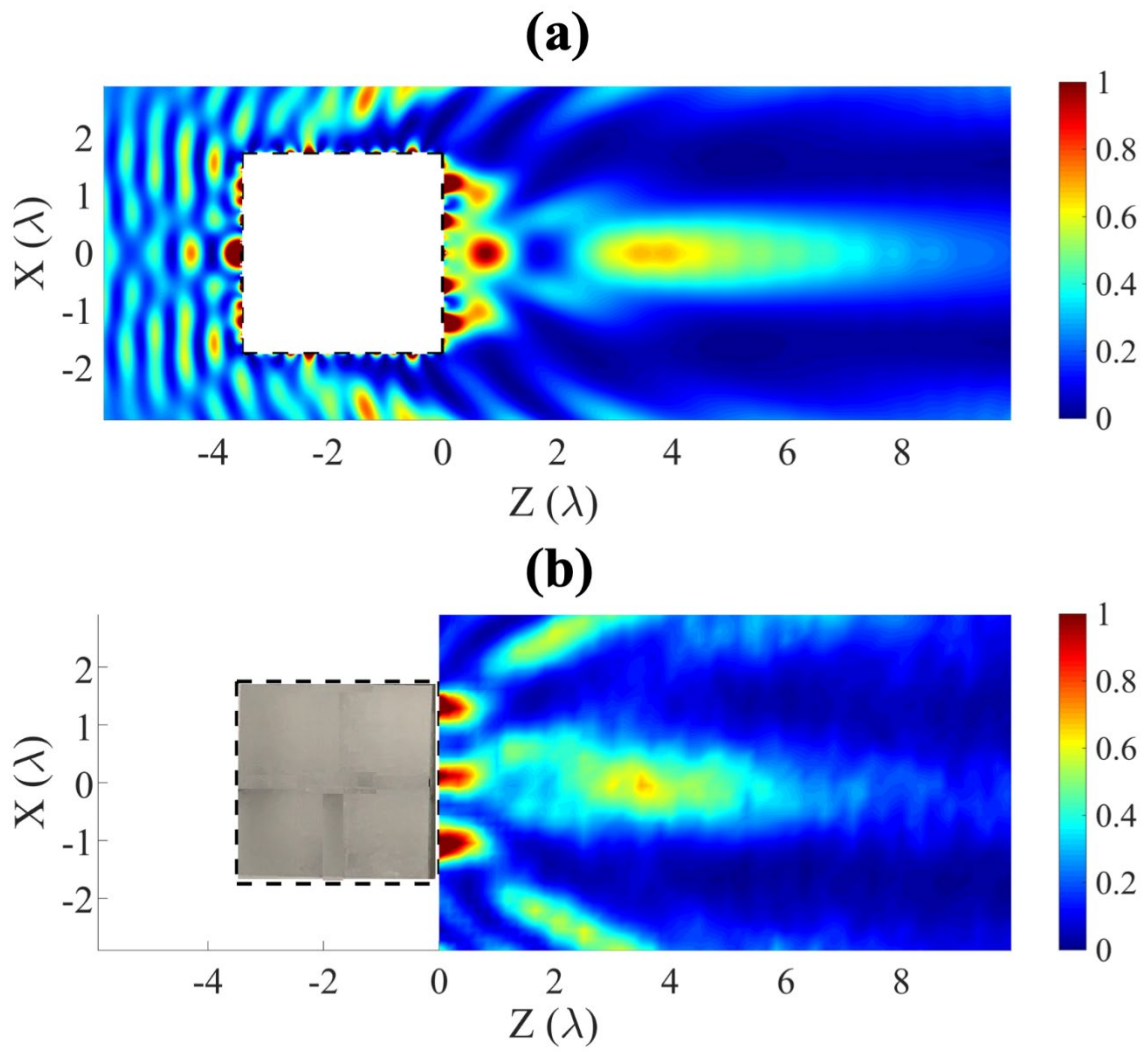


FIGURE 6

ULTRASONIC FOCUSING WITH MESOSCALE POLYMER CUBOID

Daniel Tarrazó-Serrano⁽¹⁾, Constanza Rubio^{(1)*}, Oleg V. Minin^{(2), (3)}, Antonio Uris⁽¹⁾ and Igor V. Minin^{(2), (3)}

(1) Centro de Tecnologías Físicas: Acústica, Materiales y Astrofísica, Universitat Politècnica de València, Camino de Vera s/n, 46022 Valencia, Spain

(2) Tomsk Polytechnic University, 36 Lenin Avenue, Tomsk, 634050, Russia

(3) Tomsk State University, 30 Lenin Avenue, Tomsk, 634050, Russia

* Corresponding author: E-mail: crubiom@fis.upv.es

Abstract

In this paper, we demonstrate that, contrary to what the Geometrical Optics laws dictate, a flat polymer mesoscale cuboid immersed in water with no need of negative refraction can focus sound. Two main polymers were considered and lens parameters compared: PMMA and Rexolite®. It was concluded that Rexolite® is preferable for acoustic jet formation. The nature of the formation of the foci along the longitudinal axis, that is to say along the wave propagation axis, is numerically and experimentally demonstrated. In addition, the conditions under which a cubic particles lens of this type forms a single localized region with a sub-diffraction transverse size (approximately 0.44 wavelength) are determined. The comparisons of the acoustic wave pressures and the focal distance between the Finite Element Method based numerical results and the experimental results show fair agreement.

Keywords: acoustic beam, ultrasound, polymer mesoscale cuboid

1. Introduction

In the same way as a glass convex lens focuses light, an acoustic lens can focus sound waves. A key problem with this function is a factor known as acoustic impedance. Most of modern flat acoustic lenses are made from acoustic meta-surfaces. These are flat synthetic materials designed using building blocks smaller than the wavelength of the sound.

Yang et al [1] have demonstrated that a flat acoustic lens is possible by using a closed-packed face centered-cubic array of tungsten carbide beads embedded in water. Some [2, 3, 4] of the works referred to claimed that focusing by flat lens was due to the negative refraction property [5] of the corresponding phononic crystals. In the field of acoustic, sound focusing by non-conventional optical-type lenses were reported by Kock [6].

The design a flat sub-wavelength lens that can focus acoustic wave and made from an acoustic grating with curled slits was described in [7]. A new acoustic gradient-index metasurfaces engineered from soft graded-porous silicone rubber with a high acoustic index was offered by Y. Jin et al. [8] in applications to flat acoustic lens.

In the last years, the phenomenon of optical photonic jet [9-11] has attracted great attention not only because of the scientific interest of the phenomenon, but due to its potential applications in the design of optical sensors, tools for precision surgery, among other, in optics [9, 11-12], Terahertz imaging [10, 13-15], plasmonic [16, 17], etc. A photonic jet is a narrow beam with high intensity that emerges from the shadow surface of a dielectric particle, mainly cylinder or sphere, with diameters of several wavelengths, of the incident wave, and refractive index contrast, between the material and the surrounding medium, usually less than two [9,11]. It has been demonstrated that the waist of the photonic jets can be beyond the diffraction limit by varying the refractive index contrast and the size of a sphere [9, 11].

It is well known that both acoustic and electromagnetic waves share many phenomena. Therefore, studies developed for electromagnetic waves can be extended to acoustic waves, taking into account the intrinsic differences between them. One of the most significant examples are acoustic lenses, which are currently used in different areas ranging from engineering to medicine. Like optical lenses, acoustic lenses focus sound in the same way: using the phenomenon of diffraction or refraction. Thus, as in the optical case, in acoustics there are different types of acoustic lens designs: Fresnel lenses [18-20], lenses based on sonic crystals [21, 22] or on metamaterials [23-25].

Very recently, due to the analogy between electromagnetic and acoustic waves, the idea of a phononic jet, initially developed for electromagnetic waves, has been transferred to acoustic waves. O.V. Minin and I.V. Minin [26] demonstrated for the first time, through simulations, the existence of an acoustic analogy of the photonic jet phenomenon, which they called "acoustojet" (AJ). They observed the existence of an acoustic field localization in the shadow area of a penetrable sphere. The choice of material is a key problem due to the acoustic impedance and the existence of shear wave. In the case that there is not a significant difference between the material impedance and that of the surrounding medium, the intensity of the acoustic jet will be great. If materials with a big impedance difference with the surrounding medium are used, the intensity of AJ will be relatively low but, in this case reflection from the particle is large [27]. Taking these considerations into account, if the surrounding medium is water, there are polymer materials with a slight acoustic impedance difference with respect to water, such as cross-linking polystyrene with divinyl benzene (Rexolite®) [28].

It could be noted that Rexolite®, as an acoustic water immersed lens material, is usually used for high frequency, about 20-60 MHz, showing high phase velocity (almost constant=2315 m/s) and low attenuations (almost constant =2.2 dB/mm). But the application

of such polymer for low frequency acoustic lens operating at less than 10MHz has received little attention in the literature

The experimental demonstration of the acoustojet phenomenon [28] was performed in the ultrasonic range (1.01 MHz) using a Rexolite® sphere with diameter of 8 wavelength submerged in water. The observed transverse resolution of AJ was approximately 0.52 of wavelength in the surrounding medium, which is more than the diffraction limit. In the case of a cylindrical geometry, similar experimental results were also obtained [29].

From the geometric laws of Classical Physics it is well known, that for classical lens with refractive index more than 1 the curved surfaces are required to focus sound. In recent years, the appearance of acoustic metamaterials has made possible to obtain acoustic lenses with flat surfaces. However, the mechanization of metamaterials is sometimes difficult. Therefore, it would be interesting to obtain a flat acoustic lens attained from an easily machinable natural material.

This paper presents the experimental realization of an example of underwater solid polymer acoustical lenses obtained by acoustic jet principle. Here we demonstrate that sound focusing can be obtained by flat polymer mesoscale immersed in water with no need of negative refraction. We report on measurements of a subwavelength focusing of an ultrasound beam by a polymer cubic-shaped lens immersed in water at room temperature. Due to the low acoustic impedance contrast between water and Rexolite® and taking into account the results of [28], Rexolite® has been used. Rexolite® is a thermoset plastic produced by cross linking polystyrene with divinylbenzene. It has remarkable electrical properties and is frequently used in high-frequency circuit substrates, microwave components and in red-frequency and optical devices [30, 31]. It also can be easily machined. The results obtained with Rexolite® are compared with those obtained using polymethylmethacrylate (PMMA), that is a polymer that is commonly used in the manufacture of acoustic lenses [32].

There are two areas where the acoustic field is localized along longitudinal axis by cuboid particle-lens. The different nature of these two areas is discovered, discussed and experimentally verified. The focusing capacity of the cuboid is calculated by using the Finite Element Method (FEM). Furthermore, the influence of the size of the cuboid on the focalization is analyzed numerically as a function of the incident wavelength λ . Finally, it is shown for the first time that subwavelength single field localization less than diffraction limit is possible with flat surfaces. To validate the results of the FE simulations, experimental field plots of acoustic jets have been carried out for a range of lens configurations.

2. Numerical modelling and experimental set-up

The simulation results were obtained by using the commercial software COMSOL Multiphysics Modeling©. All the FEM models were solved with 3D modeling. **This first approximation model represents the ideal case of plane wave front propagation in water, normally incident on a cuboid of solid isotropic material.** The cuboid is located in a host medium. The contours of the host medium are defined as a radiation contour. This causes Sommerfeld's condition to be fulfilled, that is, no inward reflections occur. A plane-wave traverses this medium that contains the cube. Typical density rates and water propagation rates are considered. The host medium was water with typical sound speed (c) and density (ρ) values ($c_{\text{water}} = 1500 \text{ m s}^{-1}$ and $\rho_{\text{water}} = 1000 \text{ kg m}^{-3}$). In this case, host domain was solved with "Acoustic Module". The solid mechanics module is used to define the boundary and initial conditions of the cuboid. Rexolite® cuboid domain is defined as isotropic linear elastic material, determined by its longitudinal sound speed ($c_{\text{Rexolite}} = 2337 \text{ m s}^{-1}$), shear sound speed ($c_{\text{sRexolite}} = 1157 \text{ m s}^{-1}$), and density ($\rho_{\text{Rexolite}} = 1049 \text{ kg m}^{-3}$) [25-26]. The same type of cuboid has been selected in the case of PMMA material, but with changing its longitudinal sound speed ($c_{\text{PMMA}} = 2757 \text{ m s}^{-1}$), shear sound speed ($c_{\text{sPMMA}} = 1400 \text{ m s}^{-1}$), and density

($\rho_{\text{PMMA}} = 1200 \text{ kg m}^{-3}$) [32]. To obtain a consistent solution, the multiphysics module so called «Acoustic-Structure Boundary Conditions» that solves both modules with the perfect-coupling condition has been used. The working frequency defined for the simulation is 250 kHz. Due to it is a numerical model solved in FEM, the 3D model is discretized using by tetrahedral mesh type. To avoid numerical dispersion, the maximum element size was $\lambda/8$. To validate and verify the focusing properties of the cuboid, experimental measurements were made using the ultrasonic immersion transmission technique with a total precision automated measurement system. This system consisted of a fixed-piston ultrasonic transducer used as an emitter (Imasonic, Les Savourots, France) with a central frequency of 250 kHz and an active diameter of 0.032 m. As a receiver, a polyvinylidene fluoride needle hydrophone (PVDF) (model HPM1/1, precision acoustics Ltd., Dorchester, United Kingdom) with a diameter of 1.5 mm and a bandwidth of $\pm 4 \text{ dB}$ covering from 200 kHz to 15 MHz, was used. The piston transducer emitted pulses that were detected by the hydrophone. Afterwards, the signal was acquired, post-amplified and digitalized by digital oscilloscope for PC (model 3224 of Picoscope, Pico Technology, St. Neots, United Kingdom). The spatial resolution of the scanning system was $1 \times 1 \text{ mm}^2$. During the measurements, the water temperature was 18°C and the scanning was carried out with steps of 1 mm. The Rexolite® sample measured and the experimental set-up are shown in Figure 1. The cuboid was manufactured from a Rexolite® commercially available cylinder and it was machined using a numerical control milling machine.

3. Results and discussion

First, Figure 2 shows the simulated normalized sound pressure $\frac{|P|^2}{|P_i|^2}$ distributions (where p is the sound pressure and p_i is the incident sound pressure) for Rexolite® cuboids of five different sizes in XZ planes. As can be seen in Figure 2 (a), on the shadow surface of the

cuboid side 2λ appears the AJ, this is an acoustic field enhancement with a subwavelength focus. The Full Width at Half-Maximum (FWHM) in this case is 0.44λ (or 2.64 mm), where λ is the wavelength in water, $\lambda = 6$ mm. It is important to note that such a resolution of AJ is less than the diffraction limit ($\lambda/2n = 4.7$ mm (where n is the refractive index contrast)).

As the size of the cuboid edges increases (from 2λ to 4λ with steps of 0.5λ) the position of AJ varies, as shown in Figures 2 (b) - (e). Likewise, the FWHM of AJ also increases (see Table I). **For a mesoscale cubic particle, the mechanism of focus formation is due to two main effects. First, a wave inside a cubic particle near the edge propagates with a higher phase velocity than a wave in the center of the cube. Second, there is a curvature of the normally incident plane wavefront at the edge of the cuboid. Furthermore, this curvature is such that the wave is directed into the cuboid from the edges to the center. In this case, the two maxima of these waves converge at the center, forming a focus in the form of an acoustic jet.**

To explain this phenomenon, Figure 3 shows the simulated relative intensity ($\vec{I} = p \cdot \vec{v}$, where p is the sound pressure and \vec{v} is the particle velocity) flow diagrams in XZ planes for the different sizes of the cuboid considered. Figure 3 (a) shows that there are regions where the intensity lines produce vortices, in such a way the vortices (marked with circles) near the illuminated side of the cuboid redirect the intensity flow to different areas of the cuboid. As the size of the cuboid increases (see Figure 3 (b)) the distribution of these vortices varies, resulting in a redistribution of the energy inside the cuboid. It is observed that for the cuboid of size 3λ , the convergence of the intensity flow lines is maximum in certain areas of the interior near the shadow surface of the cuboid, giving rise to the formation of jets with lower pressure, greater FWHM and greater distance from the surface of the cuboid.

Another effect that can be observed is the formation of a secondary focus in the cuboid of size 3.5λ (see Figure 2 (d)), for distances around 4λ (3.89λ) and λ (0.74λ) from the shadow side of the cuboid. This secondary focus is formed due to the interference created by

the lateral lobes of the jet that become convergent for this size of the cuboid, the path difference for these distances is zero which satisfy the constructive interference condition. These interferences produce an enhancement of the normalized sound pressure $\frac{|P|^2}{|P_i|^2}$, being 4.02 and 2.73 at λ and 4λ distance, respectively. The values of FWHM and focus length of the secondary focus located at 4λ are 1.16λ and 6.06λ respectively. Finally, for a cuboid of size 4λ , focusing effect is observed at a distance of 8λ from the shadow side of the cuboid, and hence 12λ from the “illuminated” (front) side. This effect is created by the far-field obstacle diffraction due to the interference phenomenon of the secondary sources at the “illuminated” side according to the Huygens principle. To corroborate this fact, a simulation was carried out replacing the Rexolite® cube of size 4λ with a rigid solid cube of size 4λ . To ensure that there is no propagation of waves inside the cuboid, the rigid solid condition is used. As shown in Figure 4, it is clearly seen that the focusing effect at distance 8λ is due to diffraction.

Cuboid Side (λ)	2	2.5	3	3.5	4
FWHM (λ)	0.44	0.24	0.71	0.73	0.95
Acoustic Jet Length, L (λ)	1.12	0.32	1.28	0.96	1.88
$\frac{ P_{focus} ^2}{ P_{incident} ^2}$ (Pa²)	7.2	11.1	2.9	4.1	2.1

Table I. Full Width at Half-Maximum (FWHM), Acoustic Jet length (L) and $\frac{|P_{focus}|^2}{|P_{incident}|^2}$ as a function of cuboid size.

It is interesting to note that the effect of focusing with a wavelength-scaled particle in two foci is also valid for the optical band. Wu et al [33] propose a "superlong" photonic jet was where two maxima in the distribution of the field intensity along the jet are observed. However, the nature of this effect was not fully explored [33].

For comparison with Rexolite® cuboid, PMMA cuboids of edge size 2λ and 3λ are used. Figure 5 (a)-(b) show the simulated normalized sound pressure $\frac{|P|^2}{|P_i|^2}$ distributions in XZ planes for PMMA cuboids of 2λ and 3λ size respectively. As can be observed both in Figure 5(a) and Figure 5(b), on the shadow surface of the cuboids side appear the AJ at the same position. When comparing these results with those of the Rexolite® cuboids (see Figure 2) it is observed that in the case of the PMMA cuboid of size 3λ , the AJ is on the shadow surface of particle while in the case of Rexolite® cuboid, the AJ is out of shadow surface. Moreover, in the case of 3λ edge size PMMA cuboid, the second focus (due to scattering) is more visible but for Rexolite® cuboid it is not visible. It is important if we plan to apply this particle for single-focus device. To explain this different behavior, in Figure 5 (c) - (d) it is shown, the simulated relative intensity ($\vec{I} = \vec{p} \cdot \vec{v}$) flow diagrams in XZ planes for cuboids of 2λ and 3λ size respectively. As can be seen, in the case of PMMA cuboids, the vortices are not found near the cuboid, unlike the Rexolite® cuboids, resulting in a different redistribution of the energy inside the cuboid. This fact is due to the different sound speed of the materials and more lower ratio of c_l / c_s for PMMA. So by selecting to materials properties, control of maximum pressure area position (jet) along z-axis is possible. In this case, unlike the PMMA cuboids, Rexolite® ones allow to vary the position of the maximum pressure area by varying the size of the cuboid.

To demonstrate and experimentally verify the acoustic focusing along the direction of acoustic wave propagation, we select a Rexolite® cuboid with an edge size of 3.5λ . From Figure 6 it can be seen that the simulated and experimental results agree well, which allows to validate the results of the simulations presented in this paper.

The possible discrepancies between the simulated and experimental results are due to the fact that the incident wave can not be guaranteed to be completely plane since, although

the cuboid was at a relatively long distance from the transducer, its emission is not really plane waves.

4. Conclusions

In this paper, the ultrasonic field localization produced by polymer cuboids lens immersed in water for low frequency has been investigated for the first time. As a polymer, Rexolite® has been used since it is a material with a low acoustic impedance difference with respect to water. By changing the edge size of the cuboid, it has been shown that the position of the acoustic jet varies, as does the FWHM. It has been observed and experimentally verified the appearance of effect of 2 foci farther from the cuboid and of a different nature. Such two-focusing acoustic particle-lens will greatly facilitate potential applications of far-field acoustic optics. It was also shown for the first time that it is possible to form subwavelength field localization near the shadow surface of 2λ metamaterial free cuboid lens with FWHM less than diffraction limit. The results have been compared with PMMA cuboids and it has been observed that the AJ appears at the same position on the shadow surface of the cuboids when the cuboid size varies. This effect is due to the different sound speed of the materials. So, control of maximum pressure area position along z-axis is possible by selecting to materials properties. Rexolite® is preferable polymer than PMMA in application to acoustic jet. The use of cuboids from a material such as Rexolite® is an inexpensive and easy way to obtain flat ultrasonic wavelength-scaled flat lenses. The potential applications of this type of particle-lens are varied and range from medical ultrasound to engineering applications and will be useful in the development of new ultrasonic devices, for example as a double co-propagating acoustical traps.

Acknowledgements

This work has been supported by Spanish Ministry of Science, Innovation and Universities (grant No. RTI2018-100792-B-I00). The research was partially supported by Tomsk Polytechnic University Competitiveness Enhancement Program.

References

- [1] S. Yang, J. H. Page, Z. Liu, M. L. Cowan, C. T. Chan, P. Cheng, Focusing of Sound in a 3D Phononic Crystal, *Phys. Rev. Lett.* 93 (2004), 024301.
- [2] X. Zhang, Z. Liu, Negative refraction of acoustic waves in two-dimensional phononic crystals, *Appl. Phys. Lett.* 85 (2004), 341.
- [3] L.-S. Chen, C.-H. Kuo, Z. Ye, Acoustic imaging and collimating by slabs of sonic crystals made from arrays of rigid cylinders in air, *Appl. Phys. Lett.* 85 (2004), 1072.
- [4] X. Hu, Y. Shen, X. Liu, R. Fu, J. Zi, Superlensing effect in liquid surface waves, *Phys. Rev. E* 69 (2004), 030201.
- [5] V. G. Veselago, The electrodynamics of substances with simultaneously negative values of ϵ and μ , *Sov. Phys. Usp.* 10 (1968), 509-513.
- [6] W. E. Kock, F. K. Harvey, Refracting Sound Waves, *J. Acoust. Soc. Am.* 21 (1949), 471.
- [7] P. Peng, B. Xiao, Y. Wu. Flat acoustic lens by acoustic grating with curled slits, *Phys. Lett. A*, 378(45) (2014), 3389-3392.
- [8] Y. Jin, R. Kumar, O. Poncelet, O. Mondain-Monval, T. Brunet, Flat acoustics with soft gradient-index metasurfaces, *Nat Commun.* 10 (2019), 143.
- [9] Heifetz A, Kong SC, Sahakian AV, Taflove A, Backman V, Photonic Nanojets. *J. Comput. Theor. Nanosci.* 6(9) (2009), 1979–1992.
- [10] L. Zhao, C. K. Onga, Direct observation of photonic jets and corresponding backscattering enhancement at microwave frequencies. *J. Appl. Phys.* 105 (2009), 123512.

- [11] B. S. Luk'yanchuk, R. Paniagua-Domínguez, I. V. Minin, O. V. Minin, Z. Wang, Refractive index less than two: photonic nanojets yesterday, today and tomorrow. *Opt. Mater. Express* 7 (2017), 1820-1847.
- [12] Z. Wang, W. Guo, L. Li, B. Lukyanchuk, A. Khan, Z. Liu, Z. Chen, M. Hong, Optical virtual imaging at 50 nm lateral resolution with a white-light nanoscope. *Nat. Commun.* 2 (2011), 218.
- [13] O.V. Minin, I.V. Minin, Terahertz artificial dielectric cuboid lens on substrate for super-resolution images. *Opt. Quant. Electron.* 49 (2017), 326-329.
- [14] H. H. Nguyen Pham, S. Hisatake, I.V. Minin, O.V. Minin, T. Nagatsuma, Three-dimensional direct observation of Gouy phase shift in a terajet produced by a dielectric cuboid. *Appl. Phys. Lett.* 108 (2016),191102.
- [15] H.-H. Nguyen Pham, S. Hisatake, Oleg V. Minin, T. Nagatsuma, I. V. Minin, Enhancement of Spatial Resolution of Terahertz Imaging Systems Based on Terajet Generation by Dielectric Cube. *APL Photonics* 2 (2017), 056106.
- [16] V. Pacheco-Peña, I. V. Minin, O. V. Minin, M. Beruete, Doubling the propagation distance of surface plasmon polaritons. *SPIE Newsroom* 102 (2016), 171109.
- [17] V. Pacheco-Peña, I. V. Minin, O. V. Minin, M. Beruete, Comprehensive analysis of photonic nanojets in 3D dielectric cuboids excited by surface plasmons. *Ann. Phys.* 528 (2016), 684-692.
- [18] D. C. Calvo, A. L. Thangawng, M. Nicholas, C. N. Layman, Thin Fresnel zone plate lenses for focusing underwater sound. *Appl. Phys. Lett.* 107 (2015), 114109.
- [19] X. Xia, F. Cai, F. Li, L. Meng, T. Ma, H. Zhou, M. Ke, C. Qiu, Z. Liu, H. Zheng, Planar Ultrasonic Lenses Formed by Concentric Circular Sandwiched-Ring Arrays. *Adv. Mater. Technol.* 4 (2019), 1800542.
- [20] M. Moleron, M. Serra-García, C. Daraio, Acoustic Fresnel Lenses with extraordinary transmission. *Appl. Phys. Lett.* 105 (2014), 114109.

- [21] F. Cervera, J.V. Sánchez-Pérez, R. Martínez-Sala, C. Rubio, F. Meseguer, C. Lopez, D. Caballero, J. Sánchez-Dehesa, Refractive acoustic device for airborne sound. *Phys. Rev. Lett.* 88 (2001) 023902.
- [22] A. Sukhovich, B. Merheb, K. Muralidharan, J.O.Vasseur, Y. Pennec, P.A. Deymier, J.H. Page, Experimental and Theoretical Evidence for Subwavelength Imaging in Phononic Crystals. *Phys. Rev. Lett.* 102 (2009), 154301.
- [23] Ma C, Aguinaldo, R, Liu Z, Advances in the hyperlens, *Chin. Sci. Bull.* 55 (2010), 2618.
- [24] X. Yang, J. Yin, G. Yu, L. Peng, and N. Wang, Acoustic superlens using Helmholtz-resonator-based metamaterials. *Appl. Phys. Lett.* 107 (2015),193505.
- [25] G. Y. Song, B. Huang, H. Y. Dong, Q. Cheng, T. J. Cui, Broadband Focusing Acoustic Lens Based on Fractal Metamaterials. *Sci. Rep.* 6 (2016), 35929.
- [26] O.V. Minin, I.V. Minin, Acoustic analogue of photonic jet phenomenon based on penetrable 3D particle. *Opt. Quant. Electron.* 49 (2017), 54.
- [27] J. H. Lopes, J. P. Leão-Neto, I. V. Minin, O. V. Minin, G. T. Silva, A theoretical analysis of jets. 22nd Int. Cong. Ac. (ICA 2016), Buenos Aires, 2016.
- [28] J. H. Lopes, M.A.B. Andrade, J.P. Leao-Neto, J.C. Adamowski, I.V. Minin, G.T. Silva, Focusing Acoustic Beams with a Ball-Shaped Lens beyond the Diffraction Limit. *Phys. Rev. Appl.* 8 (2017), 024013.
- [29] I.V. Minin, O.V. Minin. Mesoscale acoustical cylindrical superlenses, MATEC Web of Conferences. EDP Sciences 155 (2018), 01029
- [30] C. Cadot, J.F. Saillant, B. Dulmet, Method for Acoustic Characterization of Materials in Temperature. *Proceed. 19th World Conf. on Non-Destruc. Tes. (WCNDT)*, Munich, 2016.
- [31] Lec Plastics Inc, <http://www.rexolite.com/general-qualities/>, accessed: March, 2019.

[32] W. Xia, D. Piras, J. C. G. van Hespén, W. Steenbergen, S. Manohar, A new acoustic lens material for large area detectors in photoacoustic breast tomography. *Photoacoustics* 1 (2013), 9-18.

[33] P. Wu, J. Li, K. Wei, W. Yue, Tunable and ultra-elongated photonic nanojet generated by a liquid-immersed core-shell dielectric microsphere. *Appl. Phys Express* 8 (2015), 112001.

FIGURE CAPTIONS

Figure 1. Detail of (a) Rexolite® sample measured and (b) experimental set-up.

Figure 2. Normalized sound pressure $\frac{|p|^2}{|p_i|^2}$ distributions in XZ planes for Rexolite® cuboids different sizes: (a) 2λ , (b) 2.5λ , (c) 3λ , (d) 3.5λ and (e) 4λ

Figure 3. Normalized relative intensity flow in XZ planes for Rexolite® cuboids different sizes: (a) 2λ (the inset corresponds to an enlargement of the illuminated face of the cuboid. Vortices are indicated in the circles), and (b) 3λ

Figure 4. Normalized sound pressure $\frac{|p|^2}{|p_i|^2}$ distribution in XZ planes for a solid rigid cuboid of edge size 4λ

Figure 5. Normalized sound pressure $\frac{|p|^2}{|p_i|^2}$ distributions in XZ planes for PMMA cuboids of edge size: (a) 2λ , (b) 3λ . Normalized relative intensity flow in XZ planes for PMMA cuboids of edge size: (c) 2λ and (d) 3λ .

Figure 6. Comparison of (a) simulated and (b) measured normalized sound pressure distribution in XZ planes for Rexolite® cuboid of 3.5λ size.

TABLE

Cuboid Side (λ)	2	2.5	3	3.5	4
FWHM (λ)	0.44	0.24	0.71	0.73	0.95
Acoustic Jet Length, L (λ)	1.12	0.32	1.28	0.96	1.88
$\frac{ P_{focus} ^2}{ P_{incident} ^2}$ (Pa²)	7.2	11.1	2.9	4.1	2.1

Table I. Full Width at Half-Maximum (FWHM), acoustic jet length (L) and $\frac{|P_{focus}|^2}{|P_{incident}|^2}$.

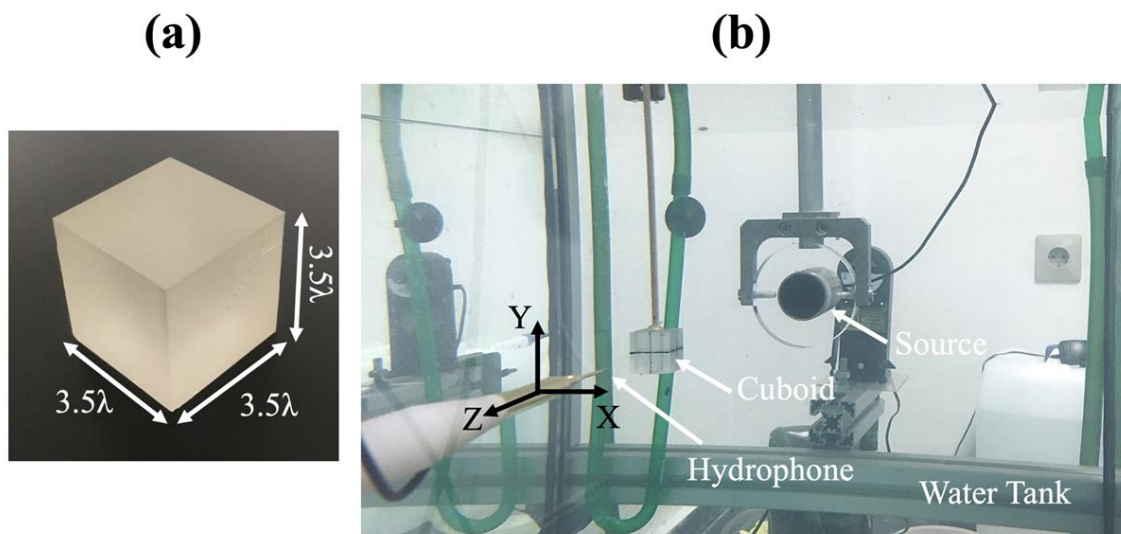


FIGURE 1

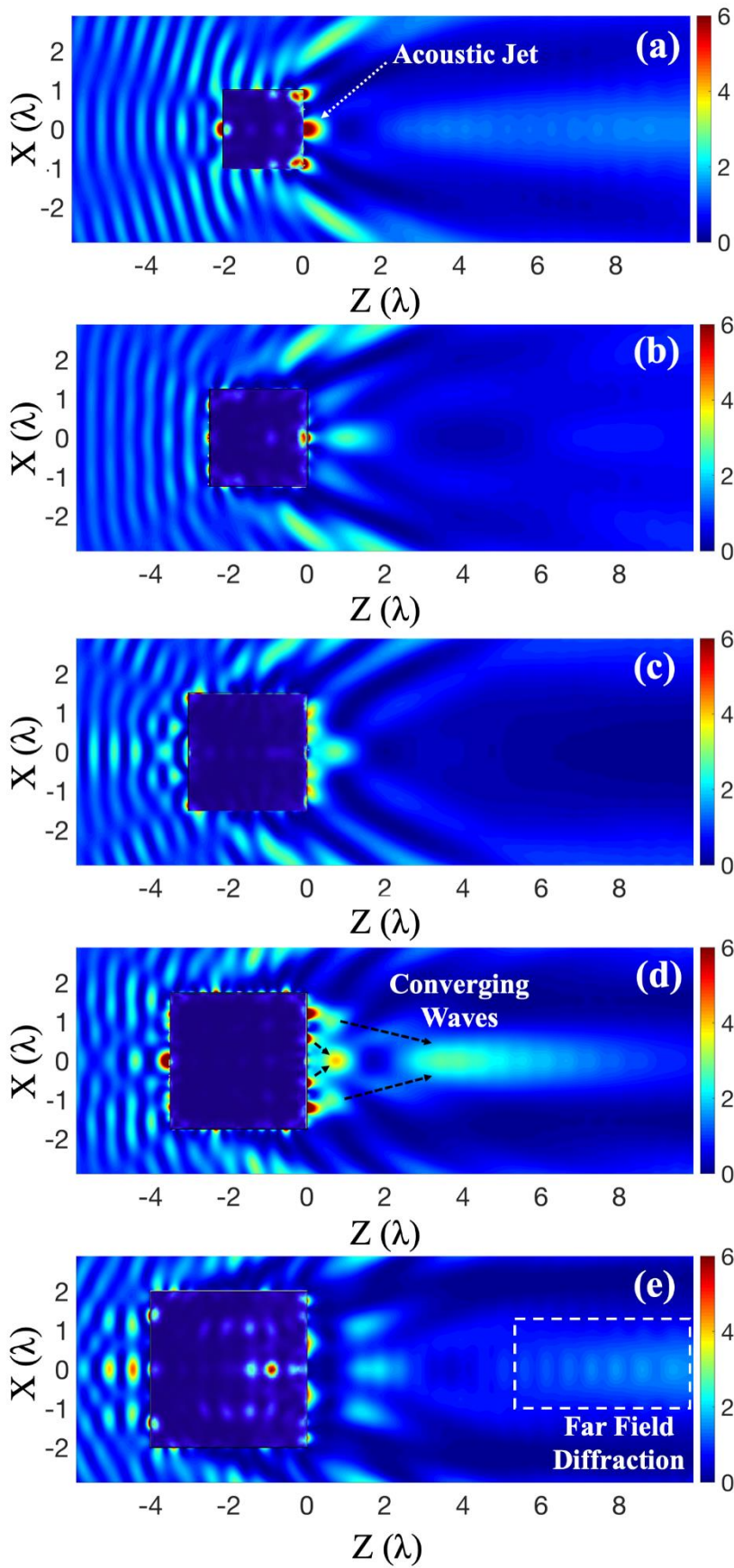


FIGURE 2

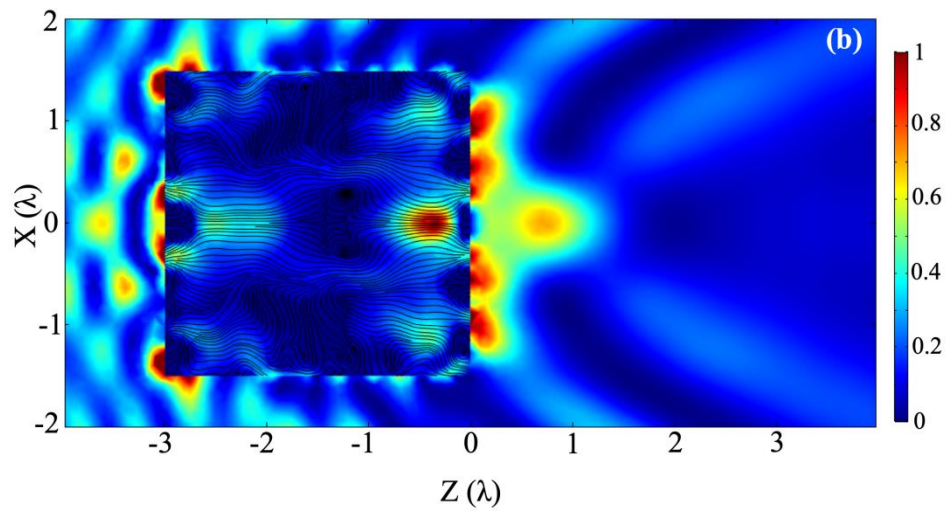
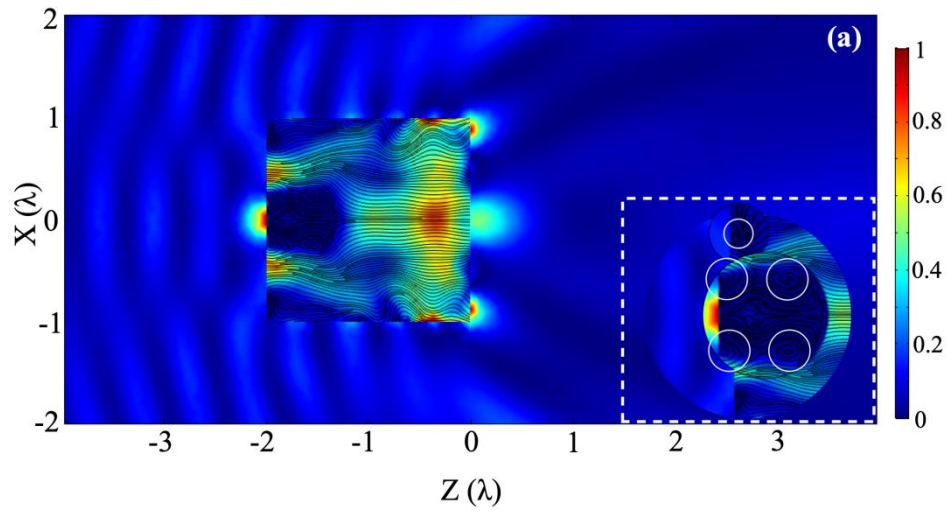


FIGURE 3

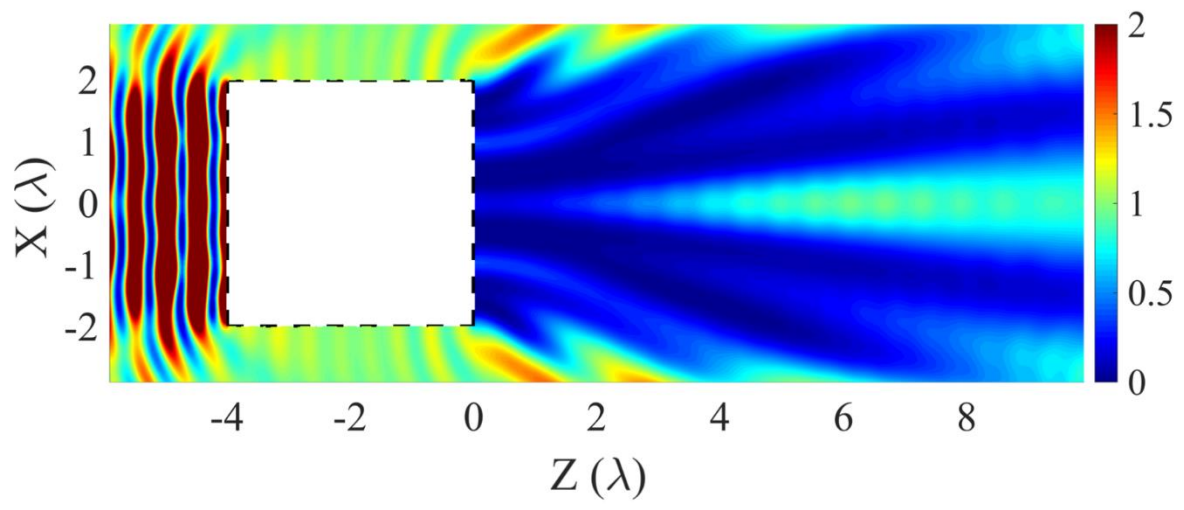


FIGURE 4

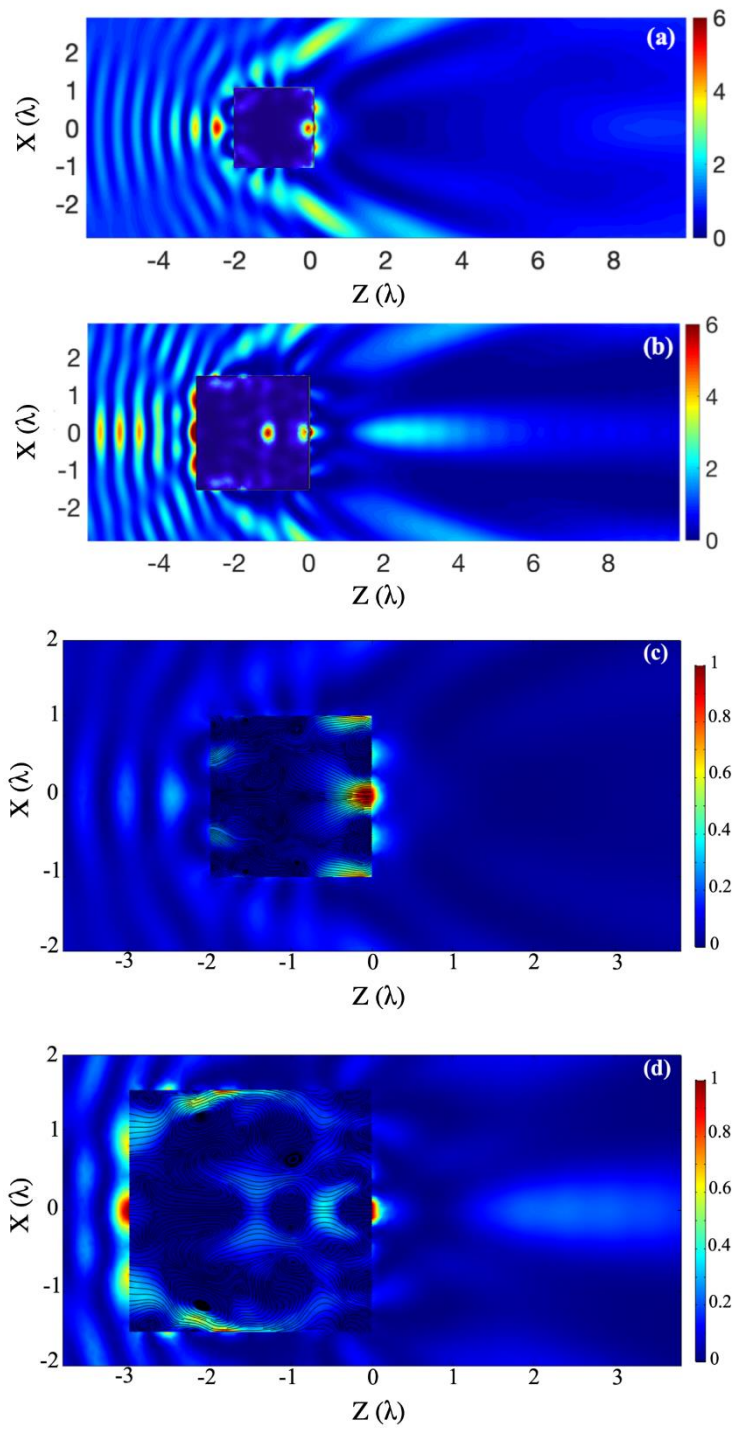


FIGURE 5

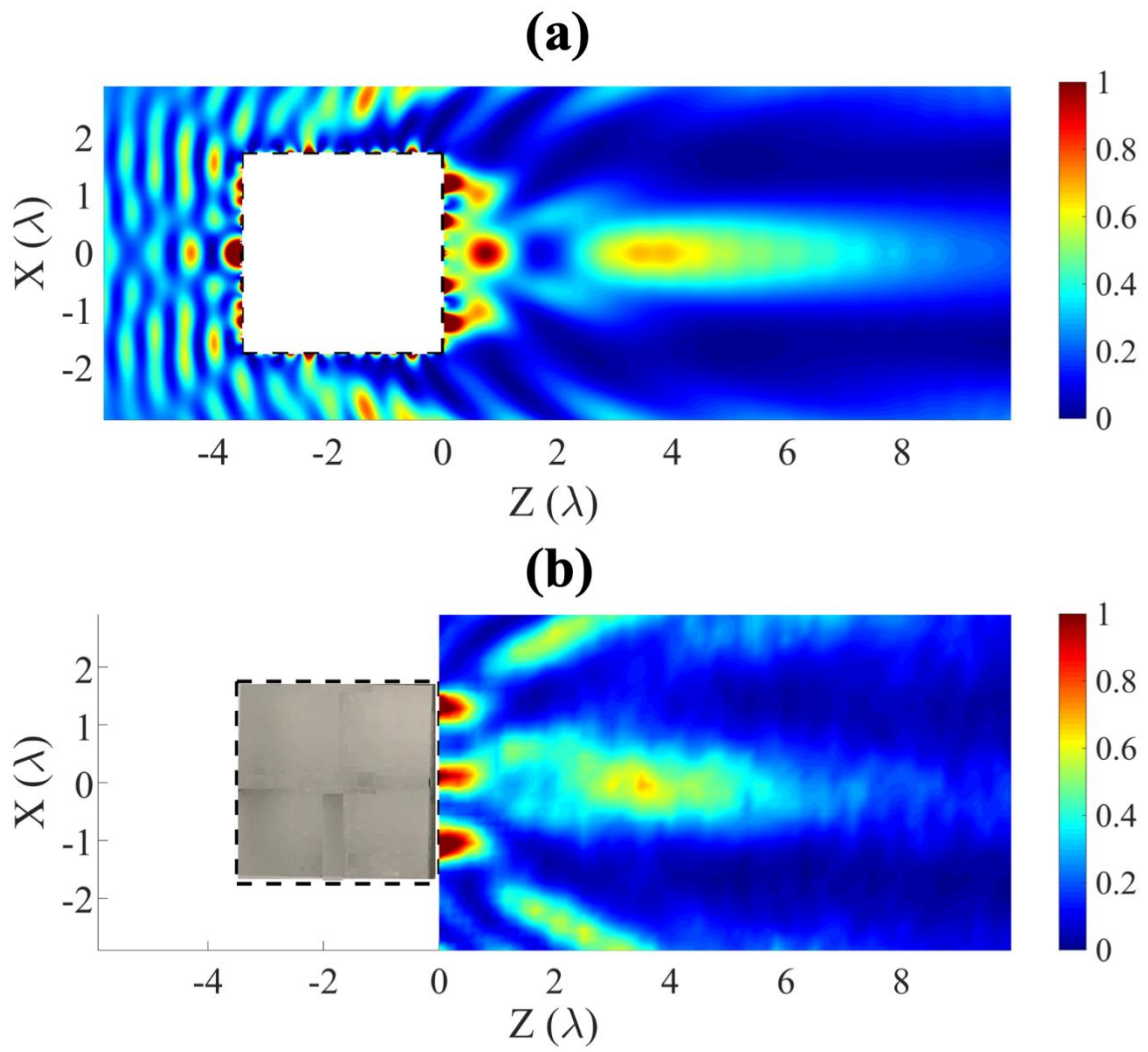


FIGURE 6